2007

Effects of General Incidence and Polymer Joining on Nucleated Polymerization in a Model of Prion Proliferation

Meredith L. Greer
Bates College, mgreer@bates.edu

P Van Den Driessche

Lin Wang

G. F. Webb

Recommended Citation
Greer, M.L., van den Driessche, P., Wang, L., Webb, G.F., 2007, Effects of General Incidence and Polymer Joining on Nucleated Polymerization in a Model of Prion Proliferation, SIAM Journal on Applied Mathematics, 68, 154-170. https://doi.org/10.1137/06066076X

SIAM J. APPL. MATH.
Vol. 68, No. 1, pp. 154–170

EFFECTS OF GENERAL INCIDENCE AND POLYMER JOINING ON NUCLEATED POLYMERIZATION IN A MODEL OF PRION PROLIFERATION*

MEREDITH L. GREER†, P. VAN DEN DRIESSCHE‡, LIN WANG§, AND G. F. WEBB¶

Abstract. Two processes are incorporated into a new model for transmissible prion diseases. These are general incidence for the lengthening process of infectious polymers attaching to and converting noninfectious monomers, and the joining of two polymers to form one longer polymer. The model gives rise to a system of three ordinary differential equations, which is shown to exhibit threshold behavior dependent on the value of the parameter combination giving the basic reproduction number $\mathcal{R}_0$. For $\mathcal{R}_0 < 1$, infectious polymers die out, whereas for $\mathcal{R}_0 > 1$, the system is locally asymptotic to a positive disease equilibrium. The effect of both general incidence and joining is to decrease the equilibrium value of infectious polymers and to increase the equilibrium value of normal monomers. Since the onset of disease symptoms appears to be related to the number of infectious polymers, both processes may significantly inhibit the course of the disease. With general incidence, the equilibrium distribution of polymer lengths is obtained and shows a sharp decrease in comparison to the distribution resulting from mass action incidence. Qualitative global results on the disease free and disease equilibria are proved analytically. Numerical simulations using parameter values from experiments on mice (reported in the literature) provide quantitative demonstration of the effects of these two processes.

Key words. prion diseases, nucleated polymerization, general incidence, polymer joining, prion proliferation

AMS subject classifications. 92D30, 34D23, 35Q80

DOI. 10.1137/06066076X

1. Introduction.

Prion diseases, though widely studied at many levels, continue to challenge understanding. A prion is an infectious protein. Several prion diseases are known, or suspected, to be transmissible, both via ingestion and iatrogenically; as a group, they are thus referred to as transmissible spongiform encephalopathies (TSEs). Examples include scrapie, which affects sheep and goats; bovine spongiform encephalopathy (BSE), which affects cows; chronic wasting disease (CWD), which affects mule deer and elk; and variant Cruetzfeldt–Jakob disease (vCJD), which affects humans [8, 9]. Additionally, mice and hamsters in laboratory experiments can be infected with scrapie [30].

Though incidence of vCJD in humans has declined to just a few new cases per year [36] and BSE incidence also appears to be declining [23], prion diseases warrant ongoing study for reasons that include the following. First, there may be previously unrecognized routes of infection: new research shows that prions can bind to some soils and cause infection via inoculation with those soils [17], indicating that graz-

*Received by the editors May 24, 2006; accepted for publication (in revised form) June 6, 2007; published electronically October 17, 2007. This work was partially supported by NSERC, MITACS, PIMS, and NSF-DMS 0516737.

http://www.siam.org/journals/siap/68-1/66076.html

†Corresponding author. Department of Mathematics, Bates College, 213 Hathorn Hall, Lewiston, ME 04240 (mgreer@bates.edu).

‡Department of Mathematics and Statistics, University of Victoria, Victoria, BC V8W 3P4, Canada (pvdd@math.uvic.ca).

§Department of Mathematics and Statistics, University of New Brunswick, Fredericton, NB E3B 5A3, Canada (lwang2@unb.ca).

¶Vanderbilt University, Department of Mathematics, 1326 Stevenson Center, Nashville, TN 37240-0001 (glenn.f.webb@vanderbilt.edu).

ing animals may acquire TSEs despite having safely prepared feed. Second, prions are extremely difficult to destroy, remaining infective despite heat or radiation that would inactivate other known infectious agents [1, 5]. Third, prion replication offers a new frontier in scientific understanding: protein-only replication cannot depend on nucleic acids, but must occur somehow for TSEs to spread. Comprehending how this replication works may provide great insight to other biological processes.

A specific naturally occurring protein is vulnerable to infection by prions; it is therefore known as prion protein. In its noninfectious form prion protein is denoted by PrP^C, and in its infectious form it is denoted by PrP^{Sc}; see, for example, [22] for discussion of this notation. The forms differ only in the folding of the protein [27]. Humans, cows, sheep, and other animals susceptible to TSEs produce PrP^C normally [4]. There is evidence both that an accumulation of PrP^{Sc} may be toxic [24, 21] and that a lack of PrP^C may leave the brain overly susceptible to stress [29]. Either or both of these may lead to symptoms associated with TSEs. In the case of transmissible prion disease, some portion of PrP^{Sc} is introduced into the system, and this PrP^{Sc} can cause more infectious protein to be made. Though the mechanism for such protein replication is not fully understood, nucleated polymerization is a likely candidate [15, 18].

Nucleated polymerization involves PrP^{Sc} attaching to PrP^C and converting it to PrP^{Sc}. While proteins usually exist as individual units, also known as monomers, it appears that PrP^{Sc} benefits from aggregating in some way [11, 16]. Aggregation confers greater stability, and may even be necessary to maintain the alternate protein folding. We assume within this paper that these aggregates have a linear form [18, 26], and we typically refer to the aggregates as polymers. In our nucleated polymerization model, each polymer may attach at either end to a PrP^C monomer, quickly converting it to the infectious form of PrP^{Sc}. Since the polymer has thus increased its length by one unit of protein, we refer to this process as *lengthening*. Nucleated polymerization also involves polymer *splitting*. We assume a minimum viable polymer length, so that when polymer splitting results in pieces below the minimum length, these pieces must break apart into their component units of PrP^C. Additionally, our model includes polymer *joining*, in which two PrP^{Sc} polymers join together to form one longer polymer.

Models of nucleated polymerization for PrP^C monomers and PrP^{Sc} polymers containing a discrete number of monomers are formulated and analyzed in [20] and [22]. Based on these, a model with continuous polymer length is introduced in [13] and further analyzed in [12, 14, 28]. All these models assume mass action incidence for the lengthening process of infectious polymers attaching to PrP^C units. We generalize this form of incidence in a way that reduces lengthening when the total amount of infectious protein becomes large in proportion to the number of polymers. Some research [24] has indicated that only truncated forms of polymers are able to lengthen this way; it is also possible that polymers within a specific range of lengths are able to lengthen at the fastest rate, but that all polymers are capable of lengthening [31]. Our general incidence term captures these features by reducing the rate of lengthening when total PrP^{Sc} mass is large relative to the total number of PrP^{Sc} polymers. That is, we reduce the rate of lengthening as the average polymer length becomes greater. In addition, our model is the first to include polymer joining. Joining is implied by the fact that large fibrils or aggregates of PrP^{Sc} are observed in late stages of disease [2, 10].

We start in section 2 by incorporating the processes of general incidence and polymer joining into an ordinary differential equation (ODE) for the number of monomers,

coupled with a partial integro-differential equation for the density of polymers depending on polymer length. Under some assumptions, this system is converted to a system of three ODEs, which is analyzed in section 3. Numerical simulations for parameters obtained from experimental data on mice [30] are presented in section 4, and we conclude in section 5 with a discussion.

2. Model formulation. A core model of nucleated polymerization exists in [12, 13, 14, 28] with some extensions in [32]. We continue to use the same variables and parameters and introduce two new parameters, ω and η, to account for general incidence and polymer joining, respectively:

- $V(t)$ is the number of $\mathrm{PrP^C}$ monomers at time t;
- $u(x,t)$ is the density of $\mathrm{PrP^{Sc}}$ polymers of length x at time t;
- x_0 is the lower bound for polymer length; that is, polymers have length x with $x_0 < x < \infty$;
- $U(t) = \int_{x_0}^{\infty} u(x,t)dx$ is the number of $\mathrm{PrP^{Sc}}$ polymers at time t;
- $P(t) = \int_{x_0}^{\infty} xu(x,t)dx$ is the number of $\mathrm{PrP^{Sc}}$ monomers comprising polymers at time t;
- $W(t) = P(t) - x_0U(t)$ is the number of $\mathrm{PrP^{Sc}}$ units not accounted for within the minimal polymer lengths;
- λ is the source rate for naturally produced $\mathrm{PrP^C}$ monomers;
- γ is the metabolic degradation rate for $\mathrm{PrP^C}$;
- τ is a rate associated with lengthening of $\mathrm{PrP^{Sc}}$ polymers by attaching to and converting $\mathrm{PrP^C}$ monomers;
- ω is a parameter associated with polymer lengthening;
- $\beta(x)$ is the length-dependent rate of polymer breakage;
- $\kappa(x,y)$ is the probability, when a polymer of length y breaks, that one of the two resulting polymers has length x;
- $\mu(x)$ is the length-dependent metabolic degradation rate of $\mathrm{PrP^{Sc}}$ polymers;
- η is the rate at which $\mathrm{PrP^{Sc}}$ polymers join together.

All parameters are assumed to be positive with the exception of ω and η, which may also be zero.

2.1. PDE model. Our model, incorporating both general incidence and polymer joining into the model formulated and discussed in [12, 13, 14, 28], has monomer dynamics governed by

$$V'(t) = \lambda - \gamma V(t) - \frac{\tau V(t)U(t)}{1+\omega P(t)} + 2\int_0^{x_0} x \int_{x_0}^{\infty} \beta(y)\kappa(x,y)u(y,t)dydx \tag{2.1}$$

with $V'(t) = \frac{dV}{dt}$, and polymer dynamics given by

$$\begin{aligned} u_t(x,t) + \frac{\tau V(t)}{1+\omega P(t)}u_x(x,t) &= -(\mu(x)+\beta(x))u(x,t) + 2\int_x^{\infty} \beta(y)\kappa(x,y)u(y,t)dy \\ &\quad + \eta\int_{x_0}^{x} u(x-y,t)u(y,t)dy - 2\eta u(x,t)\int_{x_0}^{\infty} u(y,t)dy, \end{aligned} \tag{2.2}$$

subject to nonnegative initial conditions and the boundary condition

$$u(x_0,t) = 0. \tag{2.3}$$

We write the polymer lengthening term in (2.1) in the general form $\frac{\tau V(t)U(t)}{1+\omega P(t)}$. Note that in the case $\omega = 0$ this is a mass action term. Otherwise, as $P(t)$ becomes

large there is a saturation effect, with the result that less lengthening occurs overall. This matches the in vitro observations of [24, 31].

The polymer joining term $\eta \int_{x_0}^{x} u(x-y,t)u(y,t)dy$ introduces the joining parameter η and indicates that a new polymer of length x results from the joining of two smaller polymers of lengths $x-y$ and y. Note that the upper integration limit can be written as x or $x-x_0$ with identical results, as there are zero polymers of length less than x_0. Changing the form of the integration limit does not affect analysis of the model. The last term $2\eta u(x,t)\int_{x_0}^{\infty} u(y,t)dy$ describes the loss of a polymer of length x when it joins with another polymer, of any length, to create a larger polymer. Symmetry mandates the factor 2.

Note that with mass action incidence and no polymer joining, i.e., $\omega = 0$ and $\eta = 0$, our model reduces to that in [12, 13, 14, 28]. For this case, a model with bounded $\beta(x)$, $\mu(x)$, and a general kernel $\kappa(x,y)$ is analyzed in [32].

2.2. Conversion to ODEs. Under an assumption of equidistributed splitting, a system of three ODEs in V, U, and P can be obtained from (2.1) and (2.2). Equidistributed splitting means that splitting is equally likely wherever two protein units have joined together; hence the splitting rate $\beta(x)$ is proportional to polymer length x, i.e., $\beta(x) = \beta x$. The accompanying splitting kernel is then

$$\kappa(x,y) = \begin{cases} 1/y & \text{if } y > x_0 \text{ and } 0 < x < y, \\ 0 & \text{if } y \le x_0 \text{ or } y \le x. \end{cases}$$

We make the additional assumption that polymer metabolic degradation occurs at a constant rate, i.e., $\mu(x) = \mu$. A form of the PDEs that assumes mass action and no polymer joining was converted to ODEs in [28] by integrating (2.2), and integrating the product of x and (2.2), over $[x_0, \infty)$. Proceeding similarly, the general incidence term is independent of x and converts analogously. The joining integral $\int_{x_0}^{\infty} u(x,t)\int_{x_0}^{\infty} u(y,t)dydx$ simplifies to $U^2(t)$. The remaining joining integral from (2.2) gives

$$\begin{aligned} \int_{x_0}^{\infty}\int_{x_0}^{x} u(y,t)u(x-y,t)\,dy\,dx &= \int_{x_0}^{\infty}\int_{0}^{x-x_0} u(x-z,t)u(z,t)\,dz\,dx \\ &= \int_{0}^{\infty}\int_{z+x_0}^{\infty} u(x-z,t)u(z,t)\,dx\,dz \\ &= \int_{0}^{\infty}\int_{x_0}^{\infty} u(w,t)u(z,t)\,dw\,dz \\ &= U^2(t). \end{aligned}$$

The resulting system of equations is

$$\begin{aligned} U' &= \beta P - \mu U - 2\beta x_0 U - \eta U^2, \\ V' &= \lambda - \gamma V - \frac{\tau V U}{1+\omega P} + \beta x_0^2 U, \\ P' &= \frac{\tau V U}{1+\omega P} - \mu P - \beta x_0^2 U. \end{aligned} \tag{2.4}$$

It is useful to have equations for infectious polymers, noninfectious monomers, and infectious monomers comprising polymers. To use analysis appropriate for compartmental models, we replace the U equation with an equation for $x_0 U$, and the

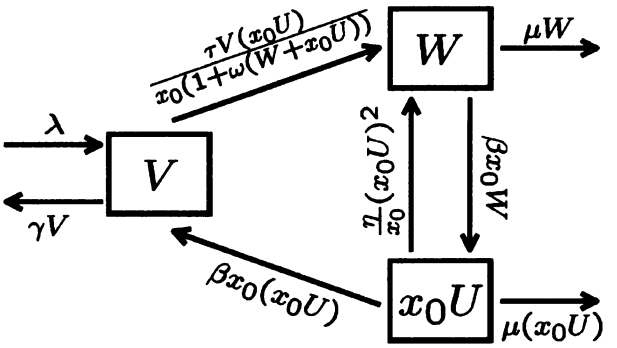

FIG. 1. *Compartmental diagram of system* (2.5).

P equation with an equation for $W = P - x_0U$. The x_0U compartment contains all PrP^{Sc} units that make up the minimum lengths of the polymers. The W compartment contains all additional PrP^{Sc} units. The resulting system of equations is

$$
\begin{aligned}
(x_0U)' &= \beta x_0 W - \mu(x_0U) - \beta x_0(x_0U) - \frac{\eta}{x_0}(x_0U)^2, \\
V' &= \lambda - \gamma V - \frac{\tau V(x_0U)}{x_0(1+\omega(W+x_0U))} + \beta x_0^2 U, \\
W' &= \frac{\tau V(x_0U)}{x_0(1+\omega(W+x_0U))} - (\mu+\beta x_0)W + \frac{\eta}{x_0}(x_0U)^2.
\end{aligned} \tag{2.5}
$$

The compartmental diagram of this system appears in Figure 1.

3. Model analysis.

3.1. Nondimensionalization. To facilitate analysis, rewrite the ODE system (2.5) in a nondimensionalized form. Let $\alpha = \mu + \beta x_0$ and $T = \alpha t$. Rewrite $U(t) = \frac{\alpha}{\tau}\mathcal{X}(T)$, $V(t) = \frac{\alpha^2}{\beta\tau}\mathcal{Y}(T)$, and $W(t) = \frac{\alpha^2}{\beta\tau}\mathcal{Z}(T)$. Define $\sigma = \frac{\beta\lambda\tau}{\alpha^3}$, $\rho = \frac{\gamma}{\alpha}$, $\delta = \frac{\beta x_0}{\alpha}$, $\nu = \frac{\omega\alpha^2}{\beta\tau}$, and $\phi = \frac{\eta}{\tau}$. Then

$$
\begin{aligned}
\mathcal{X}' &= \mathcal{Z} - \mathcal{X} - \phi\mathcal{X}^2, \\
\mathcal{Y}' &= \sigma - \rho\mathcal{Y} - \frac{\mathcal{X}\mathcal{Y}}{1+\nu(\mathcal{Z}+\delta\mathcal{X})} + \delta^2\mathcal{X}, \\
\mathcal{Z}' &= \frac{\mathcal{X}\mathcal{Y}}{1+\nu(\mathcal{Z}+\delta\mathcal{X})} - \mathcal{Z} + \delta\phi\mathcal{X}^2,
\end{aligned} \tag{3.1}
$$

with $\mathcal{X}' = \frac{d\mathcal{X}}{dT}$. The nondimensionalization process reduces the number of parameters from eight to five. Note that $\delta = \frac{\beta x_0}{\beta x_0+\mu} \in (0,1)$. Setting $\nu = 0$ simplifies the incidence term to mass action, whereas setting $\phi = 0$ simplifies the model to the case with no polymer joining.

In all that follows, disease is assumed to be initially present; thus the nonnegative initial conditions for the nondimensional system are $\mathcal{X}(0) \geq 0$, $\mathcal{Y}(0) \geq 0$, $\mathcal{Z}(0) \geq 0$, with $\mathcal{X}(0) + \mathcal{Z}(0) > 0$.

PROPOSITION 3.1. *Let* $\nu, \phi \geq 0$, $\sigma, \rho > 0$, *and* $\delta \in (0,1)$. *For each* $(\mathcal{X}(0), \mathcal{Y}(0), \mathcal{Z}(0)) \in \mathbb{R}^3_+$ *the system* (3.1) *has a unique bounded solution in* $\mathbb{R}^3_+$ *defined for all* $T \geq 0$.

Proof. Let $F : \mathbb{R}^3_+ \to \mathbb{R}^3_+$ be given by

$$F((\mathcal{X},\mathcal{Y},\mathcal{Z})) = (F_1, F_2, F_3)$$
$$= \left(\mathcal{Z} - \mathcal{X} - \phi\mathcal{X}^2, \sigma - \rho\mathcal{Y} - \frac{\mathcal{X}\mathcal{Y}}{1+\nu(\mathcal{Z}+\delta\mathcal{X})} + \delta^2\mathcal{X}, \frac{\mathcal{X}\mathcal{Y}}{1+\nu(\mathcal{Z}+\delta\mathcal{X})} - \mathcal{Z} + \delta\phi\mathcal{X}^2\right),$$

and observe that F is Lipschitz continuous on bounded sets of $\mathbb{R}^3_+$. For $T \geq 0$ and $(\mathcal{X},\mathcal{Y},\mathcal{Z}) \in \mathbb{R}^3_+$, it follows that $F_1 \geq 0$ when $\mathcal{X} = 0$, $F_2 \geq 0$ when $\mathcal{Y} = 0$, and $F_3 \geq 0$ when $\mathcal{Z} = 0$. Thus by Corollary A.5 in [35] there exists a unique nonnegative solution to (3.1) in $\mathbb{R}^3_+$ for $T \in [0,\infty)$. Since

$$\frac{d}{dT}(\delta\mathcal{X}(T) + \mathcal{Y}(T) + \mathcal{Z}(T)) = \sigma - (1-\delta)\delta\mathcal{X}(T) - \rho\mathcal{Y}(T) - (1-\delta)\mathcal{Z}(T)$$
$$\leq \sigma - \theta(\delta\mathcal{X}(T) + \mathcal{Y}(T) + \mathcal{Z}(T)),$$

where $\theta = \min\{1-\delta, \rho\} > 0$, it follows that $\delta\mathcal{X}(T) + \mathcal{Y}(T) + \mathcal{Z}(T) \leq \max\{\frac{\sigma}{\theta}, \delta\mathcal{X}(0) + \mathcal{Y}(0) + \mathcal{Z}(0)\} = M$. Thus the existence of a unique global nonnegative bounded solution is proved. □

3.2. Computing and interpreting $\mathcal{R}_0$. The disease free equilibrium (DFE) for this nondimensionalized general model of nucleated polymerization is $(\bar{\mathcal{X}},\bar{\mathcal{Y}},\bar{\mathcal{Z}}) = (0, \frac{\sigma}{\rho}, 0)$. Note that in the absence of disease, $\bar{\mathcal{Y}}$ is stable. The DFE may be used to find the basic reproduction number $\mathcal{R}_0$, which indicates the average number of new infections caused by a single infective introduced to an entirely susceptible population. One technique [37] examines the infective compartments, in this case the equations within (3.1) for $\mathcal{X}$ and $\mathcal{Z}$. The Jacobian J of the $(\mathcal{X},\mathcal{Z})$ system about the DFE is apportioned into two matrices F and G such that $J = F - G$, where F contains all elements resulting from new infections and G contains all remaining movement between compartments. Then $\mathcal{R}_0$ is the spectral radius of the matrix FG^{-1}. For the model given in (3.1),

$$F = \begin{bmatrix} 0 & 0 \\ \frac{\sigma}{\rho} & 0 \end{bmatrix}, \qquad G = \begin{bmatrix} 1 & -1 \\ 0 & 1 \end{bmatrix},$$

and the spectral radius of FG^{-1} is $\frac{\sigma}{\rho}$. Hence $\mathcal{R}_0 = \frac{\sigma}{\rho}$. The next result follows from Theorem 2 of [37].

LEMMA 3.2. *If $\mathcal{R}_0 < 1$, then the DFE of* (3.1) *is locally asymptotically stable; if $\mathcal{R}_0 > 1$, then the DFE is unstable.*

In the biological variables,

$$\mathcal{R}_0 = \frac{\beta\lambda\tau}{\gamma(\beta x_0 + \mu)^2}. \tag{3.2}$$

The same $\mathcal{R}_0$ results from the model of nucleated polymerization in which the lengthening mechanism proceeds according to mass action and polymer joining does not occur [28]. This result makes it clear that general incidence and joining do not affect the potential success of infection via nucleated polymerization. However, as shown later, the inclusion of a generalized incidence term and polymer joining does affect the distribution of polymer lengths as time progresses during disease and alters the disease equilibrium.

3.3. Global stability of the DFE. Assuming that $\rho \geq 1$, the DFE of the general model of nucleated polymerization given in (3.1) is globally attractive for $\mathcal{R}_0 \leq 1$ and globally asymptotically stable (GAS) for $\mathcal{R}_0 < 1$. The assumption that $\rho \geq 1$ is justified biologically; see data in section 4. To show the DFE results, first consider the model in the case with $\nu = 0$, that is, where polymer lengthening occurs via mass action.

LEMMA 3.3. *If* $\mathcal{R}_0 \leq 1$, *then the DFE* $(\bar{\mathcal{X}}, \bar{\mathcal{Y}}, \bar{\mathcal{Z}}) = (0, \frac{\sigma}{\rho}, 0)$ *of the system*

$$\begin{aligned} \mathcal{X}' &= \mathcal{Z} - \mathcal{X} - \phi\mathcal{X}^2, \\ \mathcal{Y}' &= \sigma - \rho\mathcal{Y} - \mathcal{X}\mathcal{Y} + \delta^2\mathcal{X}, \\ \mathcal{Z}' &= \mathcal{X}\mathcal{Y} - \mathcal{Z} + \delta\phi\mathcal{X}^2 \end{aligned} \tag{3.3}$$

is globally attractive.

Proof. Consider the Liapunov function

$$\Phi = \frac{1}{2}(\mathcal{Y} - \bar{\mathcal{Y}})^2 + k_1(\mathcal{X} + \mathcal{Z})$$

with $k_1 = (2 - \delta^2 - \bar{\mathcal{Y}})$. Since both $\delta < 1$ and $\bar{\mathcal{Y}} = \mathcal{R}_0 \leq 1$, then $k_1 > 0$. This Liapunov function is the same as that used by [28] for the nondimensionalized model with mass action and no joining. Its derivative given by

$$\Phi' = -\rho(\mathcal{Y} - \bar{\mathcal{Y}})^2 - \phi(1 - \delta)k_1\mathcal{X}^2 - \mathcal{X}[(\mathcal{Y} - 1)^2 + (1 - \delta^2)(1 - \bar{\mathcal{Y}})]$$

is nonpositive for $\mathcal{R}_0 \leq 1$. Also $\Phi' = 0$ only if $\mathcal{Y} = \bar{\mathcal{Y}}$ and $\mathcal{X} = 0$. Thus by LaSalle's invariance principle [19] the DFE $(0, \frac{\sigma}{\rho}, 0)$ of (3.3) is globally attractive. □

THEOREM 3.4. *Assume* $\rho \geq 1$. *If* $\mathcal{R}_0 \leq 1$, *then the DFE* $(\bar{\mathcal{X}}, \bar{\mathcal{Y}}, \bar{\mathcal{Z}}) = (0, \frac{\sigma}{\rho}, 0)$ *of the system* (3.1) *is globally attractive. If* $\mathcal{R}_0 < 1$, *then the DFE is GAS.*

Proof. From systems (3.1) and (3.3), create the equivalent respective systems

$$\begin{aligned} \mathcal{X}' &= \mathcal{Z} - \mathcal{X} - \phi\mathcal{X}^2, \\ \mathcal{Z}' &= \frac{\mathcal{X}(\mathcal{Y} + \mathcal{Z}) - \mathcal{X}\mathcal{Z}}{1 + \nu(\mathcal{Z} + \delta\mathcal{X})} - \mathcal{Z} + \delta\phi\mathcal{X}^2, \\ (\mathcal{Y} + \mathcal{Z})' &= \sigma - \rho(\mathcal{Y} + \mathcal{Z}) + (\rho - 1)\mathcal{Z} + \delta^2\mathcal{X} + \delta\phi\mathcal{X}^2, \end{aligned} \tag{3.4}$$

and (with $\nu = 0$)

$$\begin{aligned} \mathcal{X}' &= \mathcal{Z} - \mathcal{X} - \phi\mathcal{X}^2, \\ \mathcal{Z}' &= \mathcal{X}(\mathcal{Y} + \mathcal{Z}) - \mathcal{X}\mathcal{Z} - \mathcal{Z} + \delta\phi\mathcal{X}^2, \\ (\mathcal{Y} + \mathcal{Z})' &= \sigma - \rho(\mathcal{Y} + \mathcal{Z}) + (\rho - 1)\mathcal{Z} + \delta^2\mathcal{X} + \delta\phi\mathcal{X}^2, \end{aligned} \tag{3.5}$$

subject to the same nonnegative initial conditions. Since $\rho \geq 1$, system (3.5) is K-monotone. Then $\nu \geq 0$, $\delta \in (0,1)$, $\mathcal{X} \geq 0$, and $\mathcal{Z} \geq 0$ imply by a standard comparison theorem given in [34, Appendix B1] that $(\mathcal{X}, \mathcal{Z}, \mathcal{Y} + \mathcal{Z})_{(3.4)} \leq (\mathcal{X}, \mathcal{Z}, \mathcal{Y} + \mathcal{Z})_{(3.5)}$. Let $\mathcal{R}_0 \leq 1$. Since by Lemma 3.3, the DFE of (3.5) is globally attractive, and by Proposition 3.1, $\mathcal{X} \geq 0$ and $\mathcal{Z} \geq 0$, it follows that $\mathcal{X} \to 0$ and $\mathcal{Z} \to 0$ for system (3.4). From the second equation of (3.1), the theory of asymptotically autonomous systems [6] shows that $\mathcal{Y} \to \frac{\sigma}{\rho}$. The global asymptotic stability result then follows from Lemma 3.2. □

In order to use the comparison theorem to show that the DFE of system (3.1) is GAS, it is required that $\rho \geq 1$ in Theorem 3.4. Next we apply the Liapunov method

to establish that the DFE is GAS without assuming that $\rho \geq 1$ but at a cost: $\mathcal{R}_0$ is required to be less than $1 - \delta^2$.

THEOREM 3.5. *The DFE of system* (3.1) *is GAS if* $\mathcal{R}_0 \leq 1 - \delta^2$.

Proof. Define

$$\Phi = \mathcal{Y} - \bar{\mathcal{Y}} \ln(\mathcal{Y}/\bar{\mathcal{Y}}) + \mathcal{Z} + \mathcal{X}.$$

Notice that $\sigma = \rho\bar{\mathcal{Y}}$. The derivative of Φ along the solution of system (3.1) is given by

$$\begin{aligned}\Phi' &= -\rho\frac{(\mathcal{Y}-\bar{\mathcal{Y}})^2}{\mathcal{Y}} - (1-\delta)\phi\mathcal{X}^2 - \delta^2\bar{\mathcal{Y}}\frac{\mathcal{X}}{\mathcal{Y}} + \mathcal{X}\left(\delta^2 + \frac{\bar{\mathcal{Y}}}{1+\nu(\mathcal{Z}+\delta\mathcal{X})} - 1\right) \\ &\leq -\rho\frac{(\mathcal{Y}-\bar{\mathcal{Y}})^2}{\mathcal{Y}} - (1-\delta)\phi\mathcal{X}^2 - \delta^2\bar{\mathcal{Y}}\frac{\mathcal{X}}{\mathcal{Y}} + \mathcal{X}\left(\delta^2 + \bar{\mathcal{Y}} - 1\right).\end{aligned}$$

This shows that Φ' is nonpositive for $\mathcal{R}_0 = \frac{\sigma}{\rho} = \bar{\mathcal{Y}} < 1 - \delta^2$ and $\Phi' = 0$ only if $\mathcal{Y} = \bar{\mathcal{Y}}$ and $\mathcal{X} = 0$. Again, by LaSalle's invariance principle and Lemma 3.2, the DFE is GAS. □

3.4. Existence and stability of the EE. We now consider an endemic equilibrium (EE) with disease present, i.e., $\mathcal{X} > 0$, $\mathcal{Y} > 0$, $\mathcal{Z} > 0$.

LEMMA 3.6. *If* $\mathcal{R}_0 > 1$, *then system* (3.1) *has a unique EE. If* $\phi = 0$, *then that EE is given by* $(\mathcal{X}^*, \mathcal{Y}^*, \mathcal{Z}^*) = \left(\frac{\sigma-\rho}{\rho\nu(1+\delta)+(1-\delta^2)}, \frac{\sigma\nu(1+\delta)+(1-\delta^2)}{\rho\nu(1+\delta)+(1-\delta^2)}, \frac{\sigma-\rho}{\rho\nu(1+\delta)+(1-\delta^2)}\right)$. *If* $\mathcal{R}_0 < 1$, *then* (3.1) *has no EE.*

Proof. If $\phi > 0$, then system (3.1) cannot be solved explicitly for the EE. However, for $\phi \geq 0$, at equilibrium, $\mathcal{Z}$ and $\mathcal{Y}$ can be expressed in terms of $\mathcal{X}$ by

$$\begin{aligned}\mathcal{Z} &= \mathcal{X} + \phi\mathcal{X}^2, \\ \mathcal{Y} &= \frac{1}{\rho}\left[\sigma - \mathcal{X}(1+\phi\mathcal{X}) + \delta\mathcal{X}(\phi\mathcal{X}+\delta)\right] \\ &= \left[1 + \nu\mathcal{X}(1+\delta+\phi\mathcal{X})\right]\left[1 + \phi\mathcal{X}(1-\delta)\right],\end{aligned} \tag{3.6}$$

and $\mathcal{X}$ satisfies the cubic equation

$$\begin{aligned}0 = {} & \rho\nu\phi^2(1-\delta)\mathcal{X}^3 + \left[\rho\nu\phi + \rho\nu\phi(1-\delta^2) + \phi(1-\delta)\right]\mathcal{X}^2 \\ & + \left[\rho\nu(1+\delta) + \rho\phi(1-\delta) + (1-\delta^2)\right]\mathcal{X} + \rho - \sigma.\end{aligned} \tag{3.7}$$

Since the first three coefficients of (3.7) are positive and the constant term is negative for $\mathcal{R}_0 > 1$, there is a unique positive root. The expressions in (3.6) show that unique positive equilibrium values for $\mathcal{Y}$ and $\mathcal{Z}$ result from the unique positive $\mathcal{X}$; hence there is a unique EE $(\mathcal{X}^*, \mathcal{Y}^*, \mathcal{Z}^*)$ for $\mathcal{R}_0 > 1$. If $\phi = 0$, then the solution of (3.7) is given explicitly as $\mathcal{X}^* = \frac{\sigma-\rho}{\rho\nu(1+\delta)+(1-\delta^2)}$, giving $\mathcal{Y}^*$ and $\mathcal{Z}^*$ from (3.6) as in the lemma statement. If $\mathcal{R}_0 < 1$, then (3.7) has no positive root, and hence there is no EE. □

The proof of the following result is standard, using the Routh–Hurwitz conditions. For details, see Appendix A.

THEOREM 3.7. *If* $\mathcal{R}_0 > 1$, *then the unique EE of system* (3.1) *is locally asymptotically stable.*

Remark 3.8. If $\mathcal{R}_0 > 1$ and $\rho \geq 1$, then every solution of (3.1) approaches either the EE or the DFE.

Proof. Consider the equivalent system $(\mathcal{X}, \mathcal{Z}, \mathcal{Y}+\mathcal{Z})$ of (3.1), namely (3.4). This equivalent system's matrix of partial derivatives has the sign pattern

$$\begin{bmatrix} - & + & 0 \\ + & - & + \\ + & * & - \end{bmatrix}$$

in the case when $\rho \geq 1$ (where $*$ is $+$ or 0), indicating an irreducible cooperative system. Then by Theorems 2.3.2 and 4.1.2 on respective pages 18 and 57 of [33], the system exhibits monotone dynamical flow and solutions must approach an equilibrium. □

The system equivalent to (3.1) has only two possible equilibria: the DFE $(0, 0, \frac{\sigma}{\rho})$ and the EE $(\mathcal{X}^*, \mathcal{Z}^*, \mathcal{Y}^* + \mathcal{Z}^*)$ from Lemma 3.6. If $\mathcal{R}_0 \geq 1$, then by Lemma 3.2, the DFE is unstable, and by Theorem 3.7, the EE is locally asymptotically stable. These facts together with numerical simulations (see section 4) indicate that the EE is GAS if $\mathcal{R}_0 > 1$ and $\rho \geq 1$, but we do not have a proof.

A Liapunov function argument is used in section 3.4 of [28] to prove a global asymptotic stability result in the case $\omega = \eta = 0$.

3.5. Effects of ν and ϕ on the EE. The nucleated polymerization model with mass action and without polymer joining has been well studied in earlier work [12, 13, 14, 28]. It is useful to understand the effects of positive values of ν and ϕ on the EE of model (3.1). By taking partial derivatives of (3.6) and (3.7) and using parameter relationships at the EE, the following signs are determined. (For selected details, see Appendix B.)

PROPOSITION 3.9. *At the EE of* (3.1), *for* $\mathcal{R}_0 > 1$, $\frac{\partial \mathcal{X}^*}{\partial \nu} < 0$, $\frac{\partial \mathcal{Y}^*}{\partial \nu} > 0$, *and* $\frac{\partial \mathcal{Z}^*}{\partial \nu} < 0$.

PROPOSITION 3.10. *At the EE of* (3.1), *for* $\mathcal{R}_0 > 1$, $\frac{\partial \mathcal{X}^*}{\partial \phi} < 0$ *and* $\frac{\partial \mathcal{Y}^*}{\partial \phi} > 0$.

3.6. Summary of ODE results for biological variables. The previous results are now summarized in terms of the original biological variables in system (2.5). Recall that $\mathcal{X}$, $\mathcal{Y}$, and $\mathcal{Z}$ in (3.1) are respectively proportional to x_0U (the number of $\mathrm{PrP^{Sc}}$ units in the minimum lengths of the polymers), V (the number of $\mathrm{PrP^{C}}$ monomers), and W (the $\mathrm{PrP^{Sc}}$ units not accounted for within the minimum lengths of the polymers), all satisfying system (2.5). With nonnegative initial conditions, system (2.5) has a unique bounded solution in $\mathbb{R}^3_+$ defined for all $t \geq 0$. The basic reproduction number $\mathcal{R}_0$ is given by (3.2). The DFE $(x_0U, V, W) = (0, \frac{\lambda}{\gamma}, 0)$ is globally attractive if $\gamma \geq \beta x_0 + \mu$ and $\mathcal{R}_0 \leq 1$ and is GAS if $\mathcal{R}_0 < 1$. If $\mathcal{R}_0 > 1$ and $\gamma \geq \beta x_0 + \mu$, then the unique EE (x_0U^*, V^*, W^*) demonstrated in Lemma 3.6 is locally asymptotically stable in $\mathbb{R}^3_+ \setminus [\{0\} \times \mathbb{R}_+ \times \{0\}]$. For $\mathcal{R}_0 > 1$, at the EE, $\frac{\partial (x_0U^*)}{\partial \omega} < 0$, $\frac{\partial V^*}{\partial \omega} > 0$, $\frac{\partial W^*}{\partial \omega} < 0$, $\frac{\partial (x_0U^*)}{\partial \eta} < 0$, and $\frac{\partial V^*}{\partial \eta} > 0$. The sign of $\frac{\partial W^*}{\partial \eta}$ is undetermined in general, since the sign of $\frac{\partial \mathcal{Z}^*}{\partial \phi}$ is unknown.

We can also interpret the results in terms of P (the number of $\mathrm{PrP^{Sc}}$ monomer units comprising the polymers) from (2.4). At the DFE, $P = 0$, and at the EE, $P^* = W^* + x_0U^*$. By adding the second and third equations in (2.4), it follows that $\frac{\partial P^*}{\partial \omega} < 0$ and $\frac{\partial P^*}{\partial \eta} < 0$ at the EE. The ratio $\frac{P}{U}$ gives the mean polymer length. Dividing the last equation of (2.4) by U and differentiating with respect to η, it is seen that $\frac{d}{d\eta}\left(\frac{P^*}{U^*}\right) > 0$ at the EE.

3.7. A solution of the PDE system in the case of general incidence. Returning to (2.1) and (2.2), consider the case of general incidence but no joining,

i.e., $\eta = 0$. The corresponding system of ODEs given in system (2.4), again with $\eta = 0$, has EE from Lemma 3.6 given by the following:

$$
\begin{aligned}
U^* &= \frac{\beta\gamma(\beta x_0 + \mu)^2 - \beta^2\lambda\tau}{(2\beta x_0 + \mu)[\omega\gamma(\beta x_0 + \mu)^2 + \beta\mu\tau]}, \\
V^* &= \frac{(\beta x_0 + \mu)^2(\omega\lambda + \mu)}{\omega\gamma(\beta x_0 + \mu)^2 + \beta\mu\tau}, \\
P^* &= \frac{\gamma(\beta x_0 + \mu)^2 - \beta\lambda\tau}{\omega\gamma(\beta x_0 + \mu)^2 + \beta\mu\tau}.
\end{aligned} \tag{3.8}
$$

To find an equilibrium distribution of polymer lengths, set $\frac{\partial}{\partial t}u(x,t) = 0$ in (2.2). Compute the derivative with respect to x of the rest of (2.2), substituting in values of U^*, V^*, and P^* from (3.8) to obtain

$$
\frac{d^2}{dx^2}[u(x)] + \frac{\beta(\beta x + \mu)}{(\beta x_0 + \mu)^2}\frac{d}{dx}[u(x)] + \frac{3\beta^2}{(\beta x_0 + \mu)^2}u(x) = 0. \tag{3.9}
$$

The boundary condition $u(x_0) = 0$, first given in (2.3), can be used to find solutions to (3.9) of the form

$$
u(x) = Ce^{-\frac{\beta(x-x_0)(\beta x+\beta x_0+2\mu)}{2(\beta x_0+\mu)^2}}(x - x_0)(\beta x + \beta x_0 + 2\mu). \tag{3.10}
$$

Note that from (2.2) with $x = x_0$,

$$
\frac{d}{dx}[u(x)] = 2\beta U^*\left(\frac{1 + \omega P^*}{\tau V^*}\right). \tag{3.11}
$$

Substitute into (3.11) values of U^*, V^*, and P^* from (3.8). Then compute the derivative of (3.10) and set it equal to (3.11) to find

$$
C = \frac{\beta^3(\beta\lambda\tau - \gamma(\beta x_0 + \mu)^2)}{(\beta x_0 + \mu)^3(2\beta x_0 + \mu)[\omega\gamma(\beta x_0 + \mu)^2 + \mu\beta\tau]}.
$$

The equilibrium solution from (3.10), denoted by $u^*(x)$, is thus

$$
u^*(x) = \left(e^{-\frac{\beta(x-x_0)(\beta x+\beta x_0+2\mu)}{2(\beta x_0+\mu)^2}}\right)\frac{\beta^3(x - x_0)(\beta x + \beta x_0 + 2\mu)[\beta\lambda\tau(1 - 1/\mathcal{R}_0)]}{(\beta x_0 + \mu)^3(2\beta x_0 + \mu)[\omega\gamma(\beta x_0 + \mu)^2 + \mu\beta\tau]}, \tag{3.12}
$$

where $\mathcal{R}_0$ is given in (3.2). Note that the numerator of $u^*(x)$ requires $x > x_0$ and $\mathcal{R}_0 > 1$. The denominator of $u^*(x)$ shows that an increase in ω decreases the number of polymers of length x at steady state for all viable lengths x.

From (3.10), it can be seen that the value of x at which $u^*(x)$ achieves its maximum is independent of ω and is given by

$$
x = (\sqrt{3} - 1)\frac{\mu}{\beta} + \sqrt{3}\,x_0. \tag{3.13}
$$

However, from (3.12), the magnitude of this maximum decreases as ω increases.

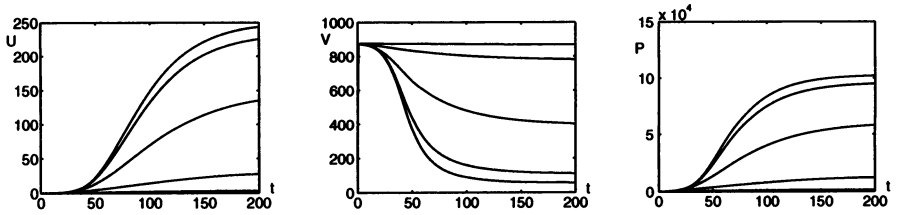

FIG. 2. *Varying* $\omega = 0, 10^{-5}, 10^{-4}, 10^{-3}, 10^{-2}$ *for populations* $U(t)$, $V(t)$, *and* $P(t)$ *with* $x_0 = 6$, $\lambda = 4400$, $\gamma = 5$, $\tau = 0.3$, $\mu = 0.04$, $\beta = 10^{-4}$, $\eta = 0$. *Range of* ω *runs top to bottom on* U *and* P *graphs, bottom to top on* V *graph.*

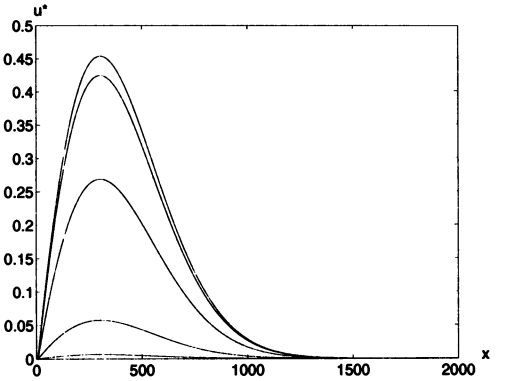

FIG. 3. *Steady-state polymer distribution* $u^*(x)$ *with* $x_0 = 6$, $\lambda = 4400$, $\gamma = 5$, $\tau = 0.3$, $\mu = 0.04$, $\beta = 10^{-4}$, $\eta = 0$, *and* $\omega = 0, 10^{-5}, 10^{-4}, 10^{-3}, 10^{-2}$. *Range of* ω *runs from top curve to bottom on graph.*

4. Numerical simulations. To complement the previous analytical results, we present some numerical simulations. All simulations shown, unless otherwise noted, use the same parameters as in [14], namely $x_0 = 6/(\text{SAF/sq})$, $\lambda = 4400/\text{day}$, $\gamma = 5/\text{day}$, $\tau = 0.3/(\text{SAF/sq} * \text{day})$, $\mu = 0.04/\text{day}$, and $\beta = 10^{-4}(\text{SAF/sq})/\text{day}$, giving $\rho \approx 2 \times 10^5 > 1$. These parameters follow from data and observations in [3, 7, 20, 25, 30]. Some broader ranges include that $x_0 \approx$ 6–30 [20], PrP^{C} has a half-life of 3–6 hours [3, 7, 25] and hence $\gamma \approx$ 3–5/day, $\mu \ll \gamma$ [20, 25], and $\lambda \approx 10^3$–10^4/day [20]. The units SAF/sq are a measure of scrapie-associated fibrils counted in spleens of Compton white mice that had been given intracerebral injections of the 139A scrapie strain [30]. Note that the above parameter set gives $\mathcal{R}_0 \approx 16$. We vary values of ω and η to investigate the changes introduced by these parameters.

First consider general incidence. The effects of the parameter ω on U, V, and P, discussed in section 3.6, are shown in Figure 2. Additionally, the equilibrium solution for $u(x)$ found in (3.12) allows a comparison of steady-state polymer distributions, given differing values of ω. This appears in Figure 3, computed from (3.12). Note that, for all values of ω, the maximum value of $u(x)$ occurs at $x \approx 303$, as can be computed from (3.13).

Next consider joining. Section 3.6 describes the effects of η on the EE of system (2.4), shown numerically in Figure 4. As discussed in section 3.6, the sign of $\frac{\partial Z^*}{\partial \phi}$ is undetermined; hence the sign of $\frac{\partial W^*}{\partial \eta}$ is also undetermined. It turns out that most parameter combinations, but not all, support $\frac{\partial Z^*}{\partial \phi} < 0$. The opposite can occur in the

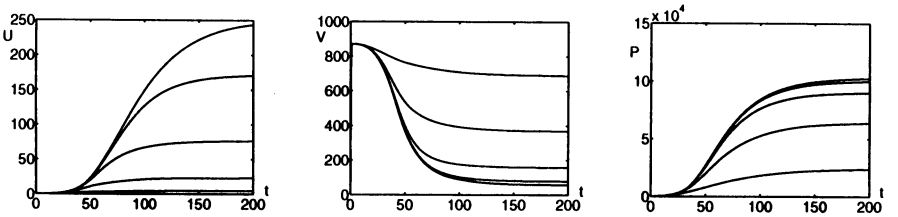

FIG. 4. *Varying* $\eta = 0, 10^{-4}, 10^{-3}, 10^{-2}, 10^{-1}$ *for populations* $U(t)$, $V(t)$, *and* $P(t)$ *with* $x_0 = 6$, $\lambda = 4400$, $\gamma = 5$, $\tau = 0.3$, $\mu = 0.04$, $\beta = 10^{-4}$, $\omega = 0$. *Range of* η *runs top to bottom on* U *and* P *graphs, bottom to top on* V *graph.*

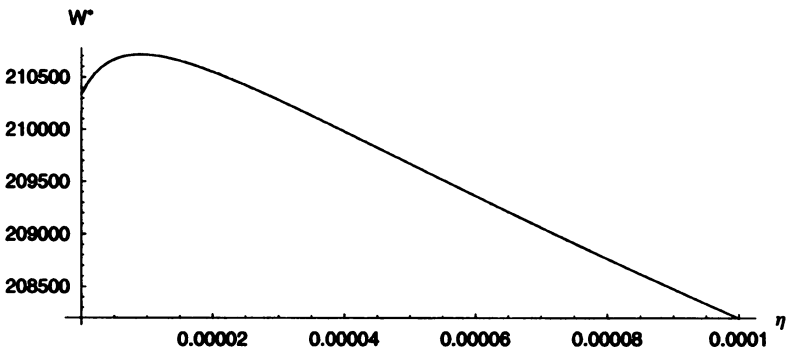

FIG. 5. *Dependence of* W^* *on* η *with* $x_0 = 6$, $\lambda = 4400$, $\gamma = 5$, $\tau = 0.3$, $\mu = 0.02$, $\beta = 10^{-4}$, $\omega = 0$.

case that $\delta \to 1$, which is possible in the case that μ is small or βx_0 is large. A brief explanation appears in Appendix C. Even so, it appears that $\frac{\partial Z^*}{\partial \phi} > 0$ for only small values of ϕ. This effect is demonstrated in Figure 5 for $\frac{\partial W^*}{\partial \eta}$, which is proportional to $\frac{\partial Z^*}{\partial \phi} > 0$. The parameters used in Figure 5 are the same as those listed above, but with smaller μ, namely $\mu = 0.02$, and $\omega = 0$.

Last, combine general incidence with joining. Lemma 3.2, Theorem 3.7, and Remark 3.8 together suggest that the EE of system (3.1) is GAS. Numerical simulations such as those shown in Figure 6 support this suggestion. The pair of surfaces in this figure show long-term equilibrium values of U and P, denoted U_∞ and P_∞, as both ω and η vary. For all shown pairs of ω and η values, both U_∞ and P_∞ remain positive, indicating (as a consequence of Remark 3.8) that they correspond to U^* and P^*. The shown ranges for ω and η correspond to the lower range of values used in Figures 2, 3, 4, and 5. Similar graphs generated using higher values of ω and η also result in positive values of U_∞ and P_∞. The parameter values used for x_0, λ, γ, τ, μ, and β are the same as those given at the beginning of this section.

Figures 2, 3, and 4 were computed using MATLAB, with `ode15s` for Figures 2 and 4. Figures 5 and 6 were computed using Mathematica.

5. Biological interpretation and discussion. We now discuss the analytical results and numerical simulations (for the assumed parameter values) in terms of prion biology. From sections 3.2 and 3.3, the system (2.4) always has a DFE $(U, V, P) = (0, \frac{\lambda}{\gamma}, 0)$, which attracts all solutions if $\gamma \geq \mu + \beta * x_0$ and $\mathcal{R}_0 = \frac{\beta\lambda\tau}{\gamma(\beta x_0 + \mu)^2} \leq 1$. This is the only equilibrium for $\mathcal{R}_0 < 1$, but for $\mathcal{R}_0 > 1$ there is a unique EE (U^*, V^*, P^*), with $P^* = W^* + x_0 U^*$ and $V^* \leq \lambda/\gamma$, as can be seen from (3.6). This equilibrium

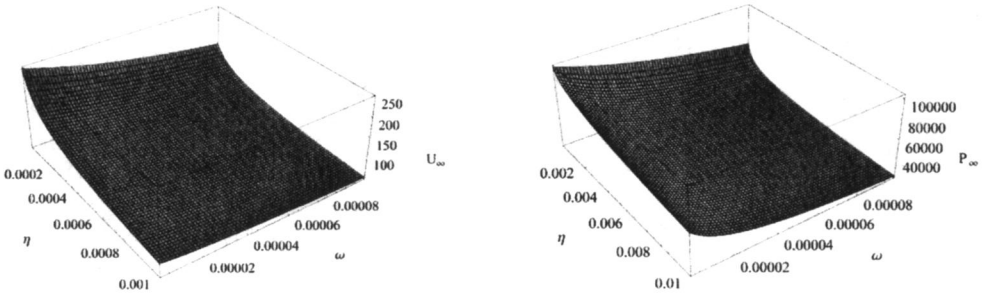

FIG. 6. *Long-term values U_∞ and P_∞ as η and ω vary. In both graphs $x_0 = 6$, $\lambda = 4400$, $\gamma = 5$, $\tau = 0.3$, $\mu = 0.04$, and $\beta = 10^{-4}$. On the U_∞ graph, $10^{-6} < \eta < 10^{-3}$, $10^{-6} < \omega < 10^{-4}$, and $50 < U_\infty < 250$. On the P_∞ graph, $10^{-6} < \eta < 10^{-2}$, $10^{-6} < \omega < 10^{-4}$, and $20,000 < P_\infty < 100,000$.*

is given explicitly by (3.8) in the case of no joining, and with joining it can be found from the solution of a cubic (see Lemma 3.6). If $\mathcal{R}_0 > 1$, then this EE is locally asymptotically stable.

From section 3.6, both increased ω and increased η cause U^* to decrease. The change related to ω indicates that as the total population of PrP^{Sc} has a greater effect on general incidence, the total number of polymers at the EE decreases. For the parameters used, if $\omega \geq 10^{-3}$, then the values of (U^*, V^*, P^*) are close to those at the DFE, as seen in Figure 2. The change related to η indicates that a higher rate of polymer joining results in fewer total polymers at the EE. Increased ω and increased η cause V^* to increase. Hence the same biological changes cause both a decrease in PrP^{Sc} polymers and an increase in PrP^{C} at the EE. Additionally, increased ω and increased η cause the equilibrium value P^* of total PrP^{Sc} to decrease. If η increases, then at the EE the mean polymer length $\frac{P^*}{U^*}$ increases, with $\ln P^*$ decreasing more slowly than $\ln U^*$.

The effects on W^* are more complicated. Increased ω, that is, increased dependence of incidence on the total PrP^{Sc} population, decreases W^*. On the other hand, an increased rate of polymer joining has a variable effect on W^*. Differing parameter combinations can cause W^* to either increase or decrease with a positive change in η; see Figure 5. That noted, it is also true that most viable parameter combinations cause W^* to decrease when η increases.

Recall that the form of $\mathcal{R}_0$ given in (3.2) is the same with either mass action or our general incidence term, and with or without polymer joining. Despite the inability of ω and η to affect disease persistence, however, each of these parameters has a demonstrable effect on the steady-state values of U, V, and P. Also, increasing ω clearly decreases the number of polymers of each possible length, with the maximum for $\omega = 10^{-4}$ being about half the maximum for $\omega = 0$; see Figure 3. From data given by Rubenstein et al. [30], the onset of symptoms of scrapie can be estimated [14] to occur as $U(t)$ reaches a critical value of 130 SAF/sq. From Figures 2 and 4, the inclusion of general incidence or joining may result in U^* less than this critical value, while V^* remains closer to its DFE value. Thus, if the effects of prion diseases are caused by either an excess of PrP^{Sc} or a lack of PrP^{C} [24, 29], then changing the EE by increasing ω or η may be enough to delay or prevent the onset of disease symptoms.

Appendix A. Proof of Theorem 3.7. Consider a system equivalent to (3.1), namely, the system given by (3.4). Setting each of the derivatives to zero gives

$$\mathcal{Z}^* = \mathcal{X}^* + \phi(\mathcal{X}^*)^2,$$
$$\frac{(\mathcal{Y}+\mathcal{Z})^* - \mathcal{Z}^*}{1+\nu(\mathcal{Z}^* + \delta\mathcal{X}^*)} = 1 + \phi(1-\delta)\mathcal{X}^*.$$

Set $q = 1 + \phi(1-\delta)\mathcal{X}^*$ and $r = 1 + \nu\mathcal{X}^*(1+\delta+\phi\mathcal{X}^*)$. Then the Jacobian of (3.4) at the unique EE is given by

$$\begin{bmatrix} -1-2\phi\mathcal{X}^* & 1 & 0 \\ 2\phi\delta\mathcal{X}^* + q - \dfrac{\nu\delta q\mathcal{X}^*}{r} & -1 - \dfrac{\mathcal{X}^*(1+\nu q)}{r} & \dfrac{\mathcal{X}^*}{r} \\ \delta^2 + 2\phi\delta\mathcal{X}^* & \rho - 1 & -\rho \end{bmatrix}.$$

The Jacobian yields the characteristic equation

$$z^3 + c_1 z^2 + c_2 z + c_3 = 0$$

with

$$c_1 = \rho + 2 + 2\phi\mathcal{X}^* + \frac{\mathcal{X}^*(1+\nu q)}{r},$$
$$c_2 = \phi\mathcal{X}^*(1-\delta) + 2\rho(1+\phi\mathcal{X}^*) + \frac{[2(1+\phi\mathcal{X}^*) + (\rho+1+\delta+2\phi\mathcal{X}^*)\nu q]\mathcal{X}^*}{r},$$
$$c_3 = (1+2\phi\mathcal{X}^*)\left(\rho + \frac{\rho\nu q\mathcal{X}^*}{r} + \frac{\mathcal{X}^*}{r}\right) - \rho\left(1 + \phi(1+\delta)\mathcal{X}^* - \frac{\delta\nu q\mathcal{X}^*}{r}\right) - \frac{\mathcal{X}^*}{r}(\delta^2 + 2\phi\delta\mathcal{X}^*).$$

Notice that $0 < \delta < 1$ and $\mathcal{X}^* > 0$ when $\mathcal{R}_0 > 1$. Clearly $c_1 > 0$ and $c_2 > 0$. Additionally,

$$c_3 > (1+2\phi\mathcal{X}^*)\left(\rho + \frac{\mathcal{X}^*}{r}\right) - \rho(1+\phi(1+\delta)\mathcal{X}^*) - \frac{\mathcal{X}^*}{r}(\delta^2 + 2\phi\delta\mathcal{X}^*) > 0.$$

Rewriting c_3 as

$$c_3 = \frac{\mathcal{X}^*}{r}[1 + 2\phi\mathcal{X}^* - (\delta^2 + 2\phi\delta\mathcal{X}^*)] + \frac{\rho\nu q\mathcal{X}^*}{r}(1 + 2\phi\mathcal{X}^* + \delta) + \rho\phi\mathcal{X}^*(1-\delta),$$

it can be shown that

$$c_1 c_2 > \frac{\mathcal{X}^*}{r}(2 + 2\phi\mathcal{X}^*) + \frac{\rho\nu q\mathcal{X}^*}{r}(2 + 2\phi\mathcal{X}^*) + \rho(2 + 2\phi\mathcal{X}^*) > c_3.$$

Hence the Routh–Hurwitz conditions are satisfied and the proof is complete. □

Appendix B. Selected proofs of Propositions 3.9 and 3.10. Differentiate (3.7) implicitly to give $\frac{\partial\mathcal{X}^*}{\partial\nu} < 0$, then compute from (3.6) that

$$\frac{\partial\mathcal{Y}^*}{\partial\nu} = -\frac{\partial\mathcal{X}^*}{\partial\nu}(1-\delta^2) - 2\phi\mathcal{X}^*\frac{\partial\mathcal{X}^*}{\partial\nu}(1-\delta) > 0.$$

Differentiate (3.7) implicitly to obtain

$$\frac{\partial \mathcal{X}^*}{\partial \phi} = \frac{-2\nu\rho\phi(1-\delta)(\mathcal{X}^*)^3 - [\nu\rho + \nu\rho(1-\delta^2) + 1 - \delta](\mathcal{X}^*)^2 - \rho(1-\delta)\mathcal{X}^*}{3\nu\rho\phi^2(1-\delta)(\mathcal{X}^*)^2 + 2[\nu\rho\phi + \nu\rho\phi(1-\delta^2) + \phi(1-\delta)]\mathcal{X}^* + \nu\rho(1+\delta) + \rho\phi(1-\delta) + 1 - \delta^2},$$

which shows that $\frac{\partial \mathcal{X}^*}{\partial \phi} < 0$. Next compute $\rho\frac{\partial \mathcal{Y}^*}{\partial \phi}$ and divide by $(1-\delta) > 0$ to find

$$\frac{\rho}{1-\delta}\frac{\partial \mathcal{Y}^*}{\partial \phi} = -2\phi\mathcal{X}\frac{\partial \mathcal{X}^*}{\partial \phi} - (\mathcal{X}^*)^2 - \frac{\partial \mathcal{X}^*}{\partial \phi}(1+\delta).$$

Substitute $\frac{\partial \mathcal{X}^*}{\partial \phi}$ from above, and write the full right-hand side over a common denominator. The resulting numerator can be simplified to give

$$\nu\rho\phi^2(1-\delta)(\mathcal{X}^*)^4 + 2\nu\rho\phi(1-\delta^2)(\mathcal{X}^*)^3 + \rho\phi(1-\delta)(\mathcal{X}^*)^2 + \nu\rho(1-\delta^2)(1+\delta)(\mathcal{X}^*)^2 + \rho(1-\delta^2)\mathcal{X}^*.$$

The numerator is seen to be strictly positive, over a positive denominator, and hence $\frac{\partial \mathcal{Y}^*}{\partial \phi} > 0$.

Appendix C. Computing values of ϕ for which $\frac{\partial \mathcal{Z}^*}{\partial \phi} > 0$. Given the EE expressions for $\mathcal{X}^*$ and $\mathcal{Z}^*$ in (3.6) and (3.7), clearly $\frac{\partial \mathcal{Z}^*}{\partial \phi} > 0$ requires that

$$\frac{\partial \mathcal{X}^*}{\partial \phi} > \frac{-(\mathcal{X}^*)^2}{2\phi\mathcal{X}^* + 1},$$

where $\frac{\partial \mathcal{X}^*}{\partial \phi}$ is given by

$$\frac{\partial \mathcal{X}^*}{\partial \phi} = \frac{-2\rho\nu\phi(1-\delta)(\mathcal{X}^*)^3 - [\rho\nu + \rho\nu(1-\delta^2) + (1-\delta)](\mathcal{X}^*)^2 - \rho(1-\delta)\mathcal{X}^*}{3\rho\nu\phi^2(1-\delta)(\mathcal{X}^*)^2 + 2[\rho\nu\phi + \rho\nu\phi(1-\delta^2) + \phi(1-\delta)]\mathcal{X}^* + \rho\nu(1+\delta) + \rho\phi(1-\delta) + 1 - \delta^2}.$$

Letting $\delta \approx 1$,

$$\frac{\partial \mathcal{X}^*}{\partial \phi} \approx -\frac{\rho\nu(\mathcal{X}^*)^2}{2\rho\nu\phi\mathcal{X}^* + 2\rho\nu} > -\frac{\rho\nu(\mathcal{X}^*)^2}{2\rho\nu\phi\mathcal{X}^* + \rho\nu} = -\frac{(\mathcal{X}^*)^2}{2\phi\mathcal{X}^* + 1}.$$

Hence for δ near 1, there are likely to be ranges of ϕ values for which $\frac{\partial \mathcal{Z}^*}{\partial \phi} > 0$.

REFERENCES

[1] T. Alper, D. A. Haig, and M. C. Clarke, *The exceptionally small size of the scrapie agent*, Biochem. Biophys. Res. Comm., 22 (1966), pp. 278–284.

[2] I. V. Baskakov, G. Legname, M. A. Baldwin, S. B. Prusiner, and F. E. Cohen, *Pathway complexity of prion protein assembly into amyloid*, J. Biol. Chem., 277 (2002), pp. 21140–21148.

[3] D. R. Borchelt, M. Scott, A. Taraboulos, N. Stahl, and S. B. Prusiner, *Scrapie and cellular prion proteins differ in their kinetics of synthesis and topology in cultured cells*, J. Cell Biol., 110 (1990), pp. 743–752.

[4] S. Brandner, S. Isenmann, A. Raeber, M. Fischer, A. Sailer, Y. Kobayashi, S. Marino, C. Weissmann, and A. Aguzzi, *Normal host prion protein necessary for scrapie-induced neurotoxicity*, Nature, 379 (1996), pp. 339–343.

[5] P. Brown, P. P. Liberski, A. Wolff, and D. C. Gajdusek, *Resistance of scrapie infectivity to steam autoclaving after formaldehyde fixation and limited survival after ashing at 360°: Practical and theoretical implications*, J. Infect. Diseases, 161 (1990), pp. 467–472.

[6] C. Castillo-Chavez and H. R. Thieme, *Asymptotically autonomous epidemic models*, in Mathematical Population Dynamics: Analysis of Heterogeneity, I. Theory of Epidemics, O. Arino, D. Axelrod, M. Kimmel, and M. Langlais, eds., Wuerz, Winnipeg, Canada, 1995, pp. 33–50.

[7] B. CAUGHEY, R. E. RACE, D. ERNST, M. J. BUCHMEIER, AND B. CHESEBRO, *Prion protein biosynthesis in scrapie-infected and uninfected neuroblastoma cells*, J. Virol., 63 (1989), pp. 175–181.

[8] J. CHIN, ED., *Control of Communicable Diseases Manual*, 17th ed., American Public Health Association, Washington, DC, 2000.

[9] CHRONIC WASTING DISEASE ALLIANCE, project website at http://www.cwd-info.org/index.php, May 17, 2006.

[10] J. H. COME, P. E. FRASER, AND P. T. LANSBURY, JR., *A kinetic model for amyloid formation in the prion diseases: Importance of seeding*, Proc. Natl. Acad. Sci. USA, 90 (1993), pp. 5959–5963.

[11] M. EIGEN, *Prionics or the kinetic basis of prion diseases*, Biophys. Chem., 63 (1996), pp. 11–18.

[12] H. ENGLER, J. PRÜSS, AND G. F. WEBB, *Analysis of a Model for the Dynamics of Prions* II, J. Math. Anal. Appl., 324 (2006), pp. 98–117.

[13] M. L. GREER, *A Population Model of Prion Dynamics*, Ph.D. Thesis, Department of Mathematics, Vanderbilt University, Nashville, TN, 2002.

[14] M. L. GREER, L. PUJO-MENJOUET, AND G. F. WEBB, *A Mathematical analysis of the dynamics of prion proliferation*, J. Theoret. Biol., 242 (2006), pp. 598–606.

[15] J. S. GRIFFITH, *Self-replication and scrapie*, Nature, 215 (1967), pp. 1043–1044.

[16] M. HORIUCHI AND B. CAUGHEY, *Prion protein interconversions and the transmissible spongiform encephalopathies*, Structure, 7 (1999), pp. R231–R240.

[17] C. J. JOHNSON, K. E. PHILLIPS, P. T. SCHRAMM, D. MCKENZIE, J. M. AIKEN, AND J. A. PEDERSEN, *Prions adhere to soil minerals and remain infectious*, Public Library of Science (PLoS) Pathogens, 2 (2006), pp. 296–302.

[18] P. T. LANSBURY AND B. CAUGHEY, *The chemistry of scrapie infection: Implications of the 'ice 9' metaphor*, Proc. Natl. Acad. Sci. USA, 92 (1995), pp. 1–5.

[19] J. P. LASALLE, *The Stability of Dynamical Systems*, CBMS-NSF Reg. Conf. Ser. Appl. Math. 25, SIAM, Philadelphia, 1976.

[20] J. MASEL, V. A. A. JANSEN, AND M. S. NOWAK, *Quantifying the kinetic parameters of prion replication*, Biophys. Chem., 77 (1999), pp. 139–152.

[21] V. NOVITSKAYA, O. V. BOCHAROVA, I. BRONSTEIN, AND I. V. BASKAKOV, *Amyloid fibrils of mammalian prion protein are highly toxic to cultured cells and primary neurons*, J. Biol. Chem., 281 (2006), pp. 13828–13836.

[22] M. A. NOWAK, D. C. KRAKAUER, A. KLUG, AND R. M. MAY, *Prion infection dynamics*, Integr. Biol., 1 (1998), pp. 3–15.

[23] OFFICE INTERNATIONAL DES EPIZOOTIES (World Organization for Animal Health), available online at http://www.oie.int/eng/info/en_esb.html, May 17, 2006.

[24] K. M. PAN, M. BALDWIN, J. NGUYEN, M. GASSET, A. SERBAN, D. GROTH, I. MEHLHORN, Z. HUANG, R. J. FLETTERICK, F. E. COHEN, AND S. B. PRUSINER, *Conversion of α-helices into β-sheets features in the formation of the scrapie prion proteins*, Proc. Natl. Acad. Sci. USA, 90 (1993), pp. 10962–10966.

[25] R. J. H. PAYNE AND D. C. KRAKAUER, *The paradoxical dynamics of prion disease latency*, J. Theoret. Biol., 191 (1998), pp. 345–352.

[26] N. PÖSCHEL, V. BRILLIANTOV, AND C. FROMMEL, *Kinetics of prion growth*, Biophys. J., 85 (2003), pp. 3460–3474.

[27] S. B. PRUSINER, *Prions*, Proc. Natl. Acad. Sci. USA, 95 (1998), pp. 13363–13383.

[28] J. PRÜSS, L. PUJO-MENJOUET, G. F. WEBB, AND R. ZACHER, *Analysis of a model for the dynamics of prions*, Discrete Contin. Dyn. Syst. Ser. B, 6 (2006), pp. 215–225.

[29] X. ROUCOU, M. GAINS, AND A. C. LEBLANC, *Neuroprotective functions of prion protein*, J. Neurosci. Res., 75 (2004), pp. 153–161.

[30] R. RUBENSTEIN, P. A. MERZ, R. J. KASCSAK, C. L. SCALICI, M. C. PAPINI, R. I. CARP, AND R. H. KIMBERLIN, *Scrapie-infected spleens: Analysis of infectivity, scrapie-associated fibrils, and protease-resistant proteins*, J. Infect. Diseases, 164 (1991), pp. 29–35.

[31] J. R. SILVEIRA, G. J. RAYMOND, A. G. HUGHSON, R. E. RACE, V. L. SIM, S. F. HAYES, AND B. CAUGHEY, *The most infectious prion protein particles*, Nature, 437 (2005), pp. 257–261.

[32] G. SIMONETT AND C. WALKER, *On the solvability of a mathematical model for prion proliferation*, J. Math. Anal. Appl., 324 (2006), pp. 580–603.

[33] H. L. SMITH, *Monotone Dynamical Systems: An Introduction to the Theory of Competitive and Cooperative Systems*, Mathematical Surveys and Monographs 41, American Mathematical Society, Providence, RI, 1995.

[34] H. L. SMITH AND P. WALTMAN, *The Theory of the Chemostat: Dynamics of Microbial Competition*, Cambridge University Press, Cambridge, UK, 1995.

[35] H. R. THIEME, *Mathematics in Population Biology*, Princeton Series in Theoret. Comput. Biol., Princeton University Press, Princeton, NJ, 2003.
[36] UK CREUTZFELDT-JAKOB DISEASE SURVEILLANCE UNIT, available online at http://www.cjd.ed.ac.uk/figures.html, May 17, 2006.
[37] P. VAN DEN DRIESSCHE AND J. WATMOUGH, *Reproduction numbers and sub-threshold endemic equilibria for compartmental models of disease transmission*, Math. Biosci., 180 (2002), pp. 29–48.